Energy-Critical Control Using Control Barrier Functions

Anil Alan, *Graduate Student Member, IEEE*, Andrej Ivanco, and Gábor Orosz, *Senior Member, IEEE*

***Abstract*—This letter proposes an energy-critical control scheme for road vehicles. The framework is designed to ensure an energy-critical goal that is defined in the form of an upper bound on the energy consumption. In order to respond to the changing traffic environment, this bound is changed based on the preceding vehicle's energy consumption. Control barrier functions are used to obtain a condition on the control input such that the energy-critical goal is formally guaranteed. This condition is used in a quadratic program scheme as a constraint, and the resulting controller intervenes the driver input in a minimally-invasive fashion. The effect of the energy-critical controller is demonstrated in data-based simulations, where up to 25% improvement in energy consumption is observed compared to an energy-inefficient driver, without drastically changing the car-following performance.**

***Index Terms*—Energy efficiency, energy filter, control barrier functions.**

I. Introduction

RELIABLE controller algorithms can be implemented on autonomous vehicles (AVs) thanks to recent technological developments. Potential benefits of these sophisticated algorithms are reported in the context of safety [1] and efficiency [2] at the vehicle level, and improved mobility and traffic throughput [3] at the societal level. Considering these positive impacts, a steady increase in the market penetration rate of AVs is expected in the near future. It is important to employ the right control strategies to take full advantage of these potentials.

Typical goals for AV control are to achieve certain performance metrics in the presence of safety constraints. Controllers with explicit control laws propose viable solutions [4], [5], [6], yet finding safe and optimal parameters for all scenarios is challenging and time consuming. A valid alternative is to formulate an optimal control framework over a finite time horizon to calculate safe and optimal trajectories [7], [8], [9], [10], [11], [12]. In a dynamic environment, though, predicting the environmental states over a horizon remains to be a major challenge. While recent end-to-end types of controllers utilize learning-based methods to mitigate model dependency [13], [14], [15], interpretability of results gets lost during the process. To resolve this issue safety filters may be utilized, which can correct the actions of performance-oriented controllers and establish formal safety guarantees [16], [17], [18], [19]. Safety filters not only separate tasks to more manageable sizes, but they also have the flexibility to be applied on any existing controller.

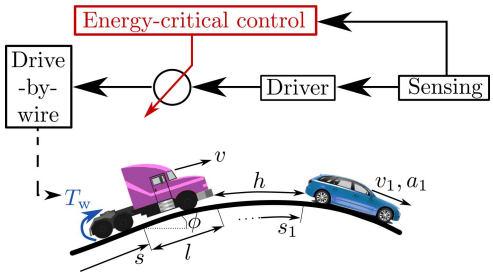

Fig. 1. The concept of energy-critical control in a car-following scenario.

In the meantime, rapidly changing market demands and regulations force manufacturers to look for guarantees regarding some of the performance metrics that have been classically considered as a part of the cost to minimize. For example, in case of electric vehicles range is a critical metric, which demands for guarantees on energy consumption. Motivated by this, our high-level goal is to propose a novel methodology for controlling the energy management of road vehicles. In particular, an energy-critical goal is defined in the form of an upper bound for consumption. With the new formulation, it is possible to obtain guarantees to complete a given task with the given amount of stored energy.

To achieve this high-level goal, our main technical contribution is to establish a control barrier function (CBF) framework which enables one to synthesize controllers that guarantee a given energy-critical performance. The key idea is to use CBFs to define a condition on the control input which ensures the forward invariance of a pre-defined set in state space [17]. While forward invariance is typically utilized for safety, here, we extend this notion to energy.

Manuscript received 15 September 2023; revised 18 November 2023; accepted 3 December 2023. Date of publication 13 December 2023; date of current version 10 January 2024. This work was supported by Allison Transmission, Inc. Recommended by Senior Editor C. Manzie. *(Corresponding author: Anil Alan.)*

Anil Alan is with the Department of Mechanical Engineering, University of Michigan, Ann Arbor, MI 48109 USA (e-mail: anilalan@umich.edu).

Andrej Ivanco is with the Data Science and Analytics, Allison Transmission, Inc., Indianapolis, IN 46222 USA (e-mail: andrej.ivanco@allisontransmission.com).

Gábor Orosz is with the Department of Mechanical Engineering and the Department of Civil and Environmental Engineering, University of Michigan, Ann Arbor, MI 48109 USA (e-mail: orosz@umich.edu).

Digital Object Identifier 10.1109/LCSYS.2023.3342771

Specifically, the CBF condition is incorporated in a quadratic program as a constraint, where the deviation from an existing (nominal) controller is penalized. The resulting controller provides us with an easy-to-implement scheme that corrects the nominal controller only when necessary. Similar to safety filters, the resulting energy filter can be applied on the top of any existing controller, including a human driver or any of those aforementioned traditional eco-driving controllers. We evaluate the performance of the proposed scheme using data-based simulations.

The organization of this letter is as follows. In Section II we present the system in consideration and formally define the energy-critical control goal. Section III, after giving a brief description of control barrier functions, introduces the energy-critical control strategy following. In Section IV we show simulation results depicting the efficacy of the energy-critical control. Section V concludes with a summary.

II. Problem Definition

Here we provide a concise description of the model utilized and the energy-critical nature of the control problem.

A. System Description

We consider the longitudinal motion of the follower in a car-following scenario; see Fig. 1. A drive-by-wire system controls the powertrain and brakes based on the position of the pedals. The dynamics are modeled as in [19]:

$$\begin{aligned} \dot{s} &= v, \\ \dot{v} &= \underbrace{\frac{T_{\mathrm{w}}}{m_{\mathrm{eff}} R}}_{u} - \underbrace{\frac{mg(\gamma_0 \cos\phi(s) + \sin\phi(s)) + k_{\mathrm{air}} v^2}{m_{\mathrm{eff}}}}_{f_{\mathrm{veh}}(s,v)}, \end{aligned} \tag{1}$$

where s is the longitudinal position of the center of gravity, while v and $\dot{v}$ are the speed and acceleration. The term T_{w} denotes the net torque acting on wheels. The torque is scaled for convenience: $u = T_{\mathrm{w}}/(m_{\mathrm{eff}}R)$, where u is measured in m/s^2. The parameters in model (1) are the mass m, the effective mass $m_{\mathrm{eff}} = m + I/R^2$, the inertia I of the rotating elements, the tire radius R, the gravitational acceleration g, the rolling resistance γ_0, and the air drag coefficient k_{air}. We use the parameter values given in Table I. The slope $\phi(s)$ changes along the road $s \in [0, s_{\mathrm{fin}}]$, where s_{fin} is the road length.

The motion of the preceding vehicle is captured by a kinematic model [19]:

$$\dot{s}_1 = v_1, \qquad \dot{v}_1 = a_1, \tag{2}$$

where s_1 is the position of the rear bumper, and v_1 and a_1 are the speed and acceleration. We assume that accurate measurements of s, v, v_1, a_1 and

$$h \triangleq s_1 - (s + l), \tag{3}$$

are available, where h is the bumper-to-bumper headway and l is the distance from the front bumper of the follower to its center of gravity. This requirement can be achieved in most modern vehicles thanks to range sensors (radar, lidar and camera) or GPS sensors and V2X connectivity.

TABLE I
Vehicle and Driver Parameters

m	5000 kg	m_{eff}	5500 kg	R	0.52 m
γ_0	0.006	k_{air}	4.1 kg/m	g	9.81 m/s^2
$u_{\min}$	-5 m/s^2	$u_{\max}$	3 m/s^2	$p_{\max}$	40 kW/ton
α	0.15 1/s	β	0.6 1/s	κ	1.3 1/s
h_{st}	7 m	τ	0.7 s		

Next, we introduce the energy consumption model. The energy consumption is defined based on the net power

$$P \triangleq P_{\mathrm{in}} - P_{\mathrm{diss}} = m_{\mathrm{eff}} v \dot{v}, \tag{4}$$

where P_{in} is the power generated by the motor/engine and P_{diss} is the dissipated power. We note that the proposed method is agnostic to the type of propulsion. In particular, we utilize the net power since it is associated with the motion, and it is possible to obtain it for the preceding vehicle using kinematic measurements without powertrain details. Furthermore, we normalize the power with the effective mass for each vehicle to obtain comparable values across vehicles having different masses; see the case depicted in Fig. 1. That is, we have

$$p \triangleq P/m_{\mathrm{eff}} = v\dot{v} = v\big(u - f_{\mathrm{veh}}(s,v)\big), \tag{5}$$

$$p_1 \triangleq v_1 a_1. \tag{6}$$

Accordingly, the energy consumption per unit mass is defined as the cumulative positive power [19]:

$$w(t) \triangleq \int_0^t \max\left\{p(\tilde{t}), 0\right\} \mathrm{d}\tilde{t}, \tag{7}$$

$$w_1(t) \triangleq \int_0^t \max\left\{p_1(\tilde{t}), 0\right\} \mathrm{d}\tilde{t}, \tag{8}$$

where the function $\max\{\cdot, 0\}$ is introduced to eliminate the negative energy consumption when vehicles decelerate.

In summary, the system is represented by the model

$$\begin{aligned} \dot{s} &= v, \\ \dot{v} &= u - f_{\mathrm{veh}}(s,v), \\ \dot{w} &= \max\big\{v\big(u - f_{\mathrm{veh}}(s,v)\big), 0\big\}, \\ \dot{h} &= v_1 - v, \\ \dot{v}_1 &= a_1, \\ \dot{w}_1 &= \max\{v_1 a_1, 0\}, \end{aligned} \tag{9}$$

which defines the state space $x \triangleq [s, v, w, h, v_1, w_1]^\top \in \mathbb{R}^6$. We assume that $s \in [0, s_{\mathrm{fin}}]$, the vehicles cannot move backward, and speed of the follower is upper bounded, i.e., $v \in [0, \bar{v}]$ and $v_1 \in \mathbb{R}_{\geq 0}$. The term $a_1 \in \mathbb{R}$ can be regarded as a known time varying external disturbance. The initial conditions are set as $s(0) = 0$, $w(0) = 0$ and $v(0)$, $h(0)$, $v_1(0)$, $w_1(0) \in \mathbb{R}_{\geq 0}$. The control input $u \in \mathbb{U}(v)$ is from the bounded set

$$\mathbb{U}(v) = \big[u_{\min}, \min\{p_{\max}/v, u_{\max}\}\big], \tag{10}$$

where $u_{\min} < 0$ corresponds to the minimum torque generated by the brakes, while $u_{\max}$ and $p_{\max}$ denote the maximum torque and power given by the powertrain. Finally, we assume

$$f_{\mathrm{veh}}(s,v) \in \mathbb{U}(v), \tag{11}$$

for all $s \in [0, s_{\text{fin}}]$ and $v \in [0, \overline{v}]$, which implies that the bounds on u do not prevent the cancellation of f_{veh}. This assumption will be used in the energy-critical control.

In the nominal system (without energy-critical control), a human driver generates the input using the pedals. Human drivers are typically modeled to respond to sensory inputs h, v and v_1 with a corresponding acceleration $a_{\text{dr}}(h, v, v_1)$. Here we use the optimal velocity model [4]:

$$a_{\text{dr}}(h, v, v_1) = \alpha\Big(\min\{\max\{\kappa(h - h_{\text{st}}), 0\}, \overline{v}\} - v\Big) + \beta(v_1 - v), \tag{12}$$

where the first term gives the acceleration associated with the range-based speed error. A linear policy is used to describe the relationship between the headway (range) and the target speed with a gradient κ. Note that the larger κ is, the more aggressive, and consequently more energy-inefficient, the follower is, since it follows the preceding vehicle with a shorter time headway. The second term gives the acceleration associated with the relative speed. Parameters are the gains α and β, and the desired stopping distance h_{st}. The time delay τ will be included as shown in Section III-C to capture the driver reaction time. Parameters used in this letter are given in Table I.

B. Energy-Critical Goal

Our goal is to establish certain energy-related guarantees that the vehicle is certified to obey all the time. Similar goals are often associated with safety, where we wish to ensure that the headway is certified to be larger than a safe distance [18]. Here we look to obtain an upper bound for the energy consumption w.

Since the controller structure offered in this letter does not consider the problem over a time horizon, employing a constant upper limit for all the time may lead to infeasible results towards the end of a run. As our goal is to maintain energy safety all along the run, we consider a variable energy-critical goal. Road conditions such as grade change, traffic lights and signs can be considered to design a proper upper bound profile. However, since the vehicle needs to respond to traffic perturbations, it may not be possible to ensure upper consumption bounds posed solely using ego vehicle states. This suggests that states of dynamic driving environment should be included to get feasible goals.

We define the energy-critical goal using the general form

$$w \leq f_{\text{eg}}(s, v, h, v_1, w_1), \tag{13}$$

where $f_{\text{eg}} : \mathbb{R}^5 \to \mathbb{R}$ is a smooth function. We first present the controller solution for the general form (13), and then we demonstrate the potential of the resulting energy-critical controller for the specific goal

$$f_{\text{eg}}(s, v, h, v_1, w_1) = cw_1, \tag{14}$$

where $c > 0$ is an arbitrary positive constant. Here, the upper bound for the consumption increases with the consumption of the preceding vehicle based on the scale determined with the parameter c. Having $c > 1$ allows the follower to consume more than the preceding vehicle while $c < 1$ requires it consume less. Thus, selecting c appropriately will enable us to avoid energy-inefficient car-following.

III. Energy-Critical Control

Since the energy-critical goal described in (13) is inspired from safety, the mathematical techniques developed for safety-critical control can be extended to energy-critical control. In particular, in this section we utilize a nonlinear controller design technique called *control barrier functions*.

A. Control Barrier Functions

Consider a general control affine nonlinear system:

$$\dot{x} = f(x) + g(x)\,u, \tag{15}$$

where $x \in \mathbb{R}^n$ are state variables with initial condition $x(0)$. Here, $u \in \mathbb{U}(x)$ is the input with the admissible control set $\mathbb{U}(x) \subseteq \mathbb{R}^m$, while $f : \mathbb{R}^n \to \mathbb{R}^n$ and $g : \mathbb{R}^n \to \mathbb{R}^{n\times m}$ are (locally Lipschitz continuous) system functions.

The concept of forward invariance of a set in the state space is defined as follows. We define $\mathcal{S}$ as the 0-superlevel set of a smooth function $b : \mathbb{R}^n \to \mathbb{R}$:

$$\mathcal{S} = \big\{x \in \mathbb{R}^n \mid b(x) \geq 0\big\}. \tag{16}$$

We assume that $\mathcal{S}$ is nonempty without any isolated points, and the gradient of b is nonzero everywhere on the boundary.

Definition 1: The set $\mathcal{S}$ is forward invariant if for any initial condition $x(0) \in \mathcal{S}$ implies $x(t) \in \mathcal{S}$ for all $t \geq 0$.

CBFs can be used to synthesize controllers that can guarantee forward invariance. Consider the following definition: A continuous function $\alpha : \mathbb{R} \to \mathbb{R}_{\geq 0}$ is class $\mathcal{K}$ ($\alpha \in \mathcal{K}$) if $\alpha(0) = 0$ and α is strictly monotonically increasing. For example, a linear function with positive gradient is class $\mathcal{K}$, i.e., $\alpha \in \mathcal{K}$ if $\alpha(r) = \alpha_c r$ with $\alpha_c > 0$.

Definition 2: The function b is a CBF for (15) on $\mathcal{S}$ if there exists an $\alpha \in \mathcal{K}$ such that the following holds for all $x \in \mathcal{S}$:

$$\sup_{u\in\mathbb{U}(x)} \Big[\underbrace{\nabla b(x) f(x)}_{L_f b(x)} + \underbrace{\nabla b(x) g(x)}_{L_g b(x)}\, u\Big] + \alpha(b(x)) \geq 0, \tag{17}$$

where $\nabla b : \mathbb{R}^n \to \mathbb{R}^n$ is the gradient of $b(x)$ w.r.t. x, and $L_f b : \mathbb{R}^n \to \mathbb{R}$ and $L_g b : \mathbb{R}^n \to \mathbb{R}^{1\times m}$ denote Lie derivatives.

Given a CBF $b(x)$ and the corresponding $\alpha \in \mathcal{K}$, we can define the set of controllers that satisfy condition (17):

$$K_{\text{CBF}}(x) = \big\{u \in \mathbb{U}(x) \big|\ L_f b(x) + L_g b(x) u \geq -\alpha(b(x))\big\}. \tag{18}$$

The existence of $b(x)$ implies that $K_{\text{CBF}}(x)$ is not empty at any point $x \in \mathcal{S}$. Now we recall the CBF theorem from [17].

Theorem 1 [17]: Let $b : \mathbb{R}^n \to \mathbb{R}$ be a CBF for (15) on $\mathcal{S}$ with an $\alpha \in \mathcal{K}$. The forward invariance of $\mathcal{S}$ is guaranteed for any (locally Lipschitz continuous) feedback controller $k : \mathbb{R}^n \to \mathbb{U}$ such that $k(x) \in K_{\text{CBF}}(x)$ for all $x \in \mathcal{S}$.

The proof is omitted for the sake of brevity, see [17].

CBFs can be incorporated in a quadratic programming (QP) to correct an existing nominal controller k_{n}:

$$k_{\text{QP}}(x) = \underset{u\in\mathbb{U}(x)}{\text{argmin}} \quad \|u - k_{\text{n}}\|^2 \quad \text{s.t.} \quad L_f b(x) + L_g b(x) u + \alpha(b(x)) \geq 0. \tag{19}$$

The constraint in the QP ensures forward invariance, while the cost function penalizes the deviation from the nominal controller. This setup ensures the forward invariance in a minimally invasive way such that the intervention only occurs when $k_n \notin K_{CBF}(x)$. Note that apart from the state x, the nominal controller may explicitly depend on various external signals and time.

If the input bounds are omitted, a closed form solution of the QP can be found[18]. Here, we give this solution for the single input case ($m = 1$) when $L_g b(x) < 0$ for all $x \in \mathcal{S}$:

$$k_{QP}(x) = \min\left\{k_n, -\frac{L_f b(x) + \alpha(b(x))}{L_g b(x)}\right\}. \tag{20}$$

In the next section we show that (20) can be implemented as an energy filter in context of the energy-critical control.

B. CBF for Energy-Critical Control

The energy-critical goal (13) suggests a CBF candidate of the form:

$$b(x) \triangleq f_{eg}(s, v, h, v_1, w_1) - w, \tag{21}$$

which defines the energy set

$$\mathcal{E} = \left\{x \in \mathbb{R}^6 \mid f_{eg}(s, v, h, v_1, w_1) - w \geq 0\right\}. \tag{22}$$

Our goal is to ensure the forward invariance of $\mathcal{E}$ w.r.t. system (9).

We remark that the car-following model (9) also has explicit time dependence through the acceleration $a_1(t)$ of the preceding vehicle, which results in $f(x, t)$ in (9). Fortunately, barrier function theory is still valid for time dependent (non-autonomous) systems; see, e.g., [20]. Another way to handle this issue is using an environmental control barrier function (ECBF) [21], which is left for future research. Here we assume that the acceleration of the preceding vehicle is bounded according to $a_1 \in [\underline{a}, \overline{a}]$.

The following theorem presents the main theoretical contribution of this letter. Here we drop the arguments of f_{eg} and f_{veh} for convenience.

Theorem 2: A function $b : \mathbb{R}^6 \to \mathbb{R}$ defined as (21) is a CBF for the system (9) if there exist a smooth function $f_{eg} : \mathbb{R}^5 \to \mathbb{R}$ and an $\alpha \in \mathcal{K}$ such that the following holds for all $x \in \mathcal{E}$ and $a_1 \in [\underline{a}, \overline{a}]$:

$$\sup_{u \in \mathbb{U}(x)} \left[\frac{\partial f_{eg}}{\partial v} u - \max\left\{v(u - f_{veh}), 0\right\}\right] \geq -\Psi(x, a_1), \tag{23}$$

where

$$\begin{aligned}\Psi(x, a_1) = \frac{\partial f_{eg}}{\partial s} v - \frac{\partial f_{eg}}{\partial v} f_{veh} + \frac{\partial f_{eg}}{\partial h}(v_1 - v) + \frac{\partial f_{eg}}{\partial v_1} a_1 \\ + \frac{\partial f_{eg}}{\partial w_1} \max\left\{v_1 a_1, 0\right\} + \alpha\big(f_{eg} - w\big).\end{aligned} \tag{24}$$

Proof: Evaluating the CBF condition (17) for b as defined in (21) towards system dynamics (9) result in (23) and (24). Thus, any smooth f_{eg} and $\alpha \in \mathcal{K}$ satisfying (23) implies that b is a CBF. ∎

Theorem 2 implies that the set of controllers

$$\begin{aligned}&K_{ECC}(x, a_1) \\ &= \left\{u \in \mathbb{U}(x) \;\middle|\; \frac{\partial f_{eg}}{\partial v} u - \max\{v(u - f_{veh}), 0\} \geq -\Psi(x, a_1)\right\}\end{aligned} \tag{25}$$

is not empty for all $x \in \mathcal{E}$ and $a_1 \in [\underline{a}, \overline{a}]$. Furthermore, Theorem 1 implies that any (locally Lipschitz continuous) controller $k : \mathbb{R}^n \times \mathbb{R} \to \mathbb{U}$ such that $k(x, a_1) \in K_{ECC}(x, a_1)$ ensures that $\mathcal{E}$ is forward invariant. The set in (25) contains the energy-critical controllers for the general energy-critical goal (13). The next corollary shows that the condition (23) is satisfied for the specific goal (14), and that in this case the set K_{ECC} can be defined with a condition affine in u.

Corollary 1: A function $b : \mathbb{R}^6 \to \mathbb{R}$ defined as in (21) with f_{eg} given in (14) with $c > 0$ is a CBF for the system (9) for any $\alpha \in \mathcal{K}$. Furthermore, we have

$$K_{ECC}(x, a_1) = \left\{u \in \mathbb{U}(x) \;\middle|\; u \leq \frac{\Psi(x, a_1)}{v} + f_{veh}\right\}, \tag{26}$$

where

$$\Psi(x, a_1) = c \max\left\{v_1 a_1, 0\right\} + \alpha\big(cw_1 - w\big). \tag{27}$$

Proof: Taking the gradient of the function f_{eg} in (14) yields

$$\nabla f_{eg}(s, v, h, v_1, w_1) = \begin{bmatrix}0 & 0 & 0 & 0 & c\end{bmatrix}^\top. \tag{28}$$

Substituting this into (23) we reformulate the condition as

$$\sup_{u \in \mathbb{U}(x)} \left[-\max\left\{v(u - f_{veh}), 0\right\}\right] \geq -\Psi(x, a_1). \tag{29}$$

Assumption (11) implies that there exists a controller $u \in \mathbb{U}(x)$ which can cancel f_{veh}. Thus, the left hand side in (29) becomes zero (notice the minus sign). Substituting (28) into (24), we obtain (27), where $-\Psi(x, a_1) \leq 0$ for all $x \in \mathcal{E}$, $a_1 \in [\underline{a}, \overline{a}]$ and $c > 0$. Thus, condition (23) is satisfied. Finally, multiplying both sides of (29) with -1 yields

$$\max\left\{v(u - f_{veh}), 0\right\} \leq \Psi(x, a_1). \tag{30}$$

Since it was previously established that $\Psi(x, a_1) \geq 0$, the left hand side is required to be bounded with a non-negative value. Therefore, dropping the $\max\{\cdot, 0\}$ does not affect the condition, and we obtain (26). Applying Theorem 2 completes the proof. ∎

Notice that the term Ψ acts as an upper limit for the power p, cf. (5) and (30). When used as a constraint in the quadratic programming (19), this limit prevents excessive power consumption in relationship to the energy-critical goal. For example, for the specific goal (14), the power limit is adjusted based on preceding vehicle's power consumption.

C. Energy Filter

Given an energy consumption bound f_{eg}, we can implement the QP in (19) to obtain an energy-critical controller that corrects the nominal controller. We refer to this as an energy filter and it is given as

$$\begin{aligned}k_{ECC}(x, a_1) = \underset{u \in \mathbb{U}(x)}{\operatorname{argmin}} \; \|u - k_n\|^2, \\ \text{s.t.} \quad \frac{\partial f_{eg}}{\partial v} u - \max\{v(u - f_{veh}), 0\} \geq -\Psi(x, a_1),\end{aligned} \tag{31}$$

where Ψ is given in (24). Notice that in general the constraint is not affine in u but for the specific goal (14) it does become affine in u; cf. (26).

Furthermore, we have a single input, and the constraint corresponds to $L_g b(x) < 0$ for $v > 0$. Therefore we can use (20), which leads to

$$k_{\mathrm{ECC}}(x, a_1) = \begin{cases} \min\left\{k_{\mathrm{n}}, \dfrac{\Psi(x, a_1)}{v} + f_{\mathrm{veh}}\right\}, & \text{if } v > 0, \\ k_{\mathrm{n}}, & \text{if } v = 0, \end{cases} \tag{32}$$

where the second case is added to avoid singularity. In our application the human driver is responsible for the nominal control input, and it is incorporated in the QP as

$$k_{\mathrm{n}} = a_{\mathrm{dr}}\big(x(t-\tau)\big) + f_{\mathrm{veh}}\big(x(t-\tau)\big). \tag{33}$$

Here a_{dr} is the desired acceleration of the driver (given by the optimal velocity model (12)), the function f_{veh} is added to compensate for the resistance terms, and the delay τ denotes the driver reaction time. Other driver models, such as the intelligent driver model [22], can be used in the nominal controller without any change in the energy filter structure. We remark that analyzing the effect of delay would require the use of a control barrier functional (CBFal) [23] but that is beyond the scope of this letter.

IV. Data-Based Simulation Results

In this section we present data-based simulation results showing the efficacy of the proposed energy-critical controller. To evaluate the controller performance in a realistic scenario we incorporate road data in the simulations. Car-following experiments were conducted with two human-driven vehicles along a 25-km segment of a public road ($s_{\mathrm{fin}} = 25$ km). GPS sensors recorded the position, speed and acceleration of the vehicles. These experiments were repeated 10 times.

The speed profile of the preceding vehicle is depicted in the top panel of Fig. 2, where the average speed of all runs is shown as a solid black curve, and the standard deviation is depicted by gray shading. Traffic lights and traffic congestion were the main causes of the variations between different runs. Such variation is in fact desirable to evaluate the energy-critical control in a dynamic environment.

We use the data corresponding to the follower vehicle to obtain a set of model parameters that matches with the driving characteristics; see Table I. The corresponding time profiles are depicted in Fig. 2 with slight discrepancy in headway, which is deemed negligible for our purpose. The energy-inefficient nature of the driving arise from the large value of $\kappa = 1.3$ 1/s. In order to evaluate the robustness of the method for other types of driver characteristics we also create a 'cautious' driver by setting $\kappa = 0.7$ 1/s.

The controller (32) with (27) is utilized using the linear class $\mathcal{K}$ function $\alpha(r) = \alpha_c r$ with gain $\alpha_c = 1$ 1/s. First, we show a sequence of events showcasing the efficacy of the controller in ensuring the energy-critical goal for $c = 1$. The energy consumption and power profiles are depicted in Fig. 3. Black dashed-dotted curves represent the preceding vehicle, red curves depict the energy-inefficient driver, and green curves show the energy-critical controller (ECC). Unlike

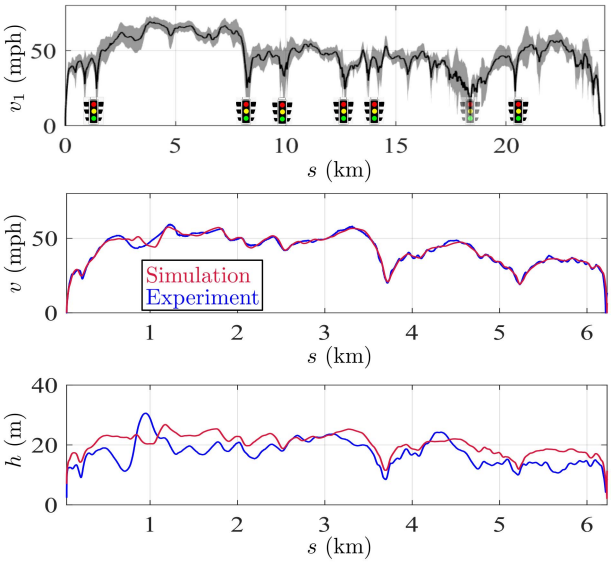

Fig. 2. (Top) Average and standard deviation of the preceding vehicle's speed as a function of the travelled distance. (Middle and bottom) Comparison between the experimental data (blue) and the simulation data (red) with the energy-inefficient driver model given in (12) and Table I.

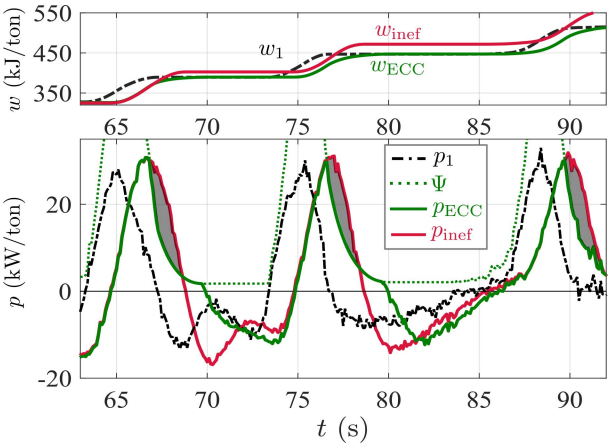

Fig. 3. Energy consumption and power profiles of the energy-inefficient human driver (red) and the energy-critical controller (green) for $c = 1$. The data for the preceding vehicle is shown by black dash-dotted curves. The shaded regions highlight the energy gain.

the energy-inefficient driver, ECC never violates $w \le f_{\mathrm{eg}} = w_1$. When the preceding vehicle starts decelerating, Ψ decreases in accordance with preceding vehicle's power p_1, and the ECC intervenes. The energy gain is highlighted by the shaded regions in the bottom panel. In fact, although both systems are at the same consumption level at $t = 65$ seconds, after three braking incidents the ECC consumes 5% less at $t = 90$ seconds.

Next, we present simulation results using all preceding vehicle driving profiles for different values of the parameter $c \in [0.75, 1.25]$. For all simulations we use the same initial conditions and conclude at the same destination. To capture the car-following performance we use a headway-based drivability metric: $h_{\mathrm{index}} \triangleq \frac{1}{s_{\mathrm{fin}}} \int_0^{s_{\mathrm{fin}}} h(s)\, \mathrm{d}s$, where $h(s)$ denotes the headway as a function of travelled distance. This headway index corresponds to the (Lagrangian) average headway over

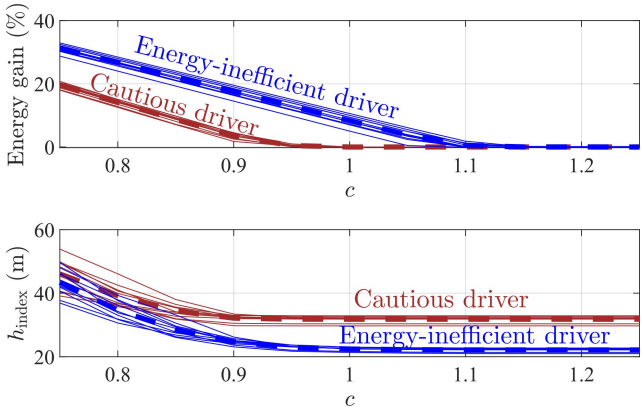

Fig. 4. Energy gain (top) and headway index (bottom) for various c values.

the road. Thus, keeping h_{index} as small as possible can improve the traffic throughput.

The results are given in Fig. 4, where the top panel depicts the energy gain for both the energy-inefficient driver ($\kappa = 1.3$ 1/s) and the cautious driver ($\kappa = 0.7$ 1/s). Solid curves show the results for individual preceding vehicle driving profiles, and thick dashed curves mark the averages. A linear relationship between the energy gain and c arises below a c value. This value is observed to be smaller for the cautious driver, because this driver tends to make more energy-efficient decisions, therefore there is much less behavior to filter. In the meantime, the relationship between c and h_{index} is observed to have parabolic characteristics for smaller c. In summary, applying the ECC may lead up to 25% gain in energy with the expense $\sim$5 m increase in average headway.

The results given in Fig. 4 suggest that an optimization framework can be constructed to find the best c. Such framework may be adapted for a time varying c, where an online algorithm updates c based on the driving characteristics of the human driver and on the preceding vehicle's profile. Establishing such a scheme is left for future work.

V. Conclusion

In this letter, we proposed an energy-critical control scheme in a car-following scenario. After describing the system model, we introduced the energy-critical goal. The CBF framework was utilized to obtain a condition satisfying the goal. The condition was used in a QP to design an energy filter. The obtained energy-critical controller intervened the nominal controller to enforce the energy-critical goal. The efficacy of the controller was demonstrated using data-based numerical simulations, where 20-40% increase in energy efficiency was observed without drastically changing the car-following performance. Future work includes updating the energy-critical goal based on environmental data, and implementing the energy filter in an experimental setup.

References

[1] T. Ersal et al., "Connected and automated road vehicles: State of the art and future challenges," *Veh. Syst. Dyn.*, vol. 58, no. 5, pp. 672–704, 2020.

[2] A. Vahidi and A. Sciarretta, "Energy saving potentials of connected and automated vehicles," *Transp. Res. C, Emerg. Technol.*, vol. 95, pp. 822–843, Oct. 2018.

[3] S. S. Avedisov, G. Bansal, and G. Orosz, "Impacts of connected automated vehicles on freeway traffic patterns at different penetration levels," *IEEE Trans. Intell. Transp. Syst.*, vol. 23, no. 5, pp. 4305–4318, May 2022.

[4] G. Orosz, "Connected cruise control: Modelling, delay effects, and nonlinear behaviour," *Veh. Syst. Dyn.*, vol. 54, no. 8, pp. 1147–1176, 2016.

[5] Z. Li, W. Li, S. Xu, and Y. Qian, "Stability analysis of an extended intelligent driver model and its simulations under open boundary condition," *Physica A Stat. Mech. Appl.*, vol. 419, pp. 526–536, Feb. 2015.

[6] C. Lu, J. Dong, and L. Hu, "Energy-efficient adaptive cruise control for electric connected and autonomous vehicles," *IEEE Intell. Transp. Syst. Mag.*, vol. 11, no. 3, pp. 42–55, Jul. 2019.

[7] H. Borhan, A. Vahidi, A. M. Phillips, M. L. Kuang, I. V. Kolmanovsky, and S. Di Cairano, "MPC-based energy management of a power-split hybrid electric vehicle," *IEEE Trans. Control Syst. Technol.*, vol. 20, no. 3, pp. 593–603, May 2012.

[8] M. Shen, R. A. Dollar, T. G. Molnar, C. R. He, A. Vahidi, and G. Orosz, "Energy-efficient reactive and predictive connected cruise control," *IEEE Trans. Intell. Veh.*, early access, May 31, 2023, doi: 10.1109/TIV.2023.3281763.

[9] D. D. Yoon, B. Ayalew, A. Ivanco, and Y. Chen, "Predictive kinetic energy management for large electric vehicles using radar information," in *Proc. IEEE Conf. Control Technol. Appl. (CCTA)*, 2020, pp. 82–87.

[10] T. Ard, L. Guo, J. Han, Y. Jia, A. Vahidi, and D. Karbowski, "Energy-efficient driving in connected corridors via minimum principle control: Vehicle-in-the-loop experimental verification in mixed fleets," *IEEE Trans. Intell. Veh.*, vol. 8, no. 2, pp. 1279–1291, Feb. 2023.

[11] S. Kousik, S. Vaskov, F. Bu, M. Johnson-Roberson, and R. Vasudevan, "Bridging the gap between safety and real-time performance in receding-horizon trajectory design for mobile robots," *Int. J. Robot. Res.*, vol. 39, no. 12, pp. 1419–1469, 2020.

[12] B. Groelke, C. Earnhardt, J. Borek, and C. Vermillion, "A predictive command governor-based adaptive cruise controller with collision avoidance for non-connected vehicle following," *IEEE Trans. Intell. Transp. Syst.*, vol. 23, no. 8, pp. 12276–12286, Aug. 2022.

[13] J. Wang, Y. Zheng, Q. Xu, and K. Li, "Data-driven predictive control for connected and autonomous vehicles in mixed traffic," in *Proc. Amer. Control Conf. (ACC)*, 2022, pp. 4739–4745.

[14] S. Kuutti, R. Bowden, Y. Jin, P. Barber, and S. Fallah, "A survey of deep learning applications to autonomous vehicle control," *IEEE Trans. Intell. Transp. Syst.*, vol. 22, no. 2, pp. 712–733, Feb. 2021.

[15] D. Shen, J. Han, D. Karbowski, and A. Rousseau, "Data-driven design of model predictive control for powertrain-aware eco-driving considering nonlinearities using Koopman analysis," *IFAC-PapersOnLine*, vol. 55, no. 24, pp. 117–122, 2022.

[16] P. Nilsson et al., "Correct-by-construction adaptive cruise control: Two approaches," *Trans. Control Syst. Technol.*, vol. 24, no. 4, pp. 1294–1307, 2015.

[17] A. D. Ames, X. Xu, J. W. Grizzle, and P. Tabuada, "Control barrier function based quadratic programs for safety critical systems," *IEEE Trans. Autom. Control*, vol. 62, no. 8, pp. 3861–3876, Aug. 2017.

[18] A. Alan, A. J. Taylor, C. R. He, A. D. Ames, and G. Orosz, "Control barrier functions and input-to-state safety with application to automated vehicles," *IEEE Trans. Control Syst. Technol.*, vol. 31, no. 6, pp. 2744–2759, Nov. 2023.

[19] A. Alan, C. R. He, T. G. Molnar, J. C. Mathew, A. H. Bell, and G. Orosz, "Integrating safety with performance in connected automated truck control: Experimental validation," *IEEE Trans. Intell. Veh.*, early access, Aug. 15, 2023, doi: 10.1109/TIV.2023.3305204.

[20] A. Alan, T. G. Molnar, A. D. Ames, and G. Orosz, "Parameterized barrier functions to guarantee safety under uncertainty," *IEEE Control Syst. Lett.*, vol. 7, pp. 2077–2082, Jun. 2023.

[21] T. G. Molnar, A. K. Kiss, A. D. Ames, and G. Orosz, "Safety-critical control with input delay in dynamic environment," *IEEE Trans. Control Syst. Technol.*, vol. 31, no. 4, pp. 1507–1520, Jul. 2023.

[22] A. Kesting, M. Treiber, and D. Helbing, "Enhanced intelligent driver model to access the impact of driving strategies on traffic capacity," *Philosoph. Trans. Roy. Soc. A*, vol. 368, no. 1928, pp. 4585–4605, 2010.

[23] A. K. Kiss, T. G. Molnar, A. D. Ames, and G. Orosz, "Control barrier functionals: Safety-critical control for time delay systems," *Int. J. Robust Nonlinear Control*, vol. 33, no. 12, pp. 7282–7309, 2023.